Observation of strained PdO in an aged Pd/ceria–zirconia catalyst

G.W. Graham [a], A.E. O'Neill [a,*], D. Uy [a], W.H. Weber [a], H. Sun [b], and X.Q. Pan [b]

[a] Ford Research Laboratory, MD3179/SRL, P.O. Box 2053, Dearborn, MI 48121, USA
[b] Department of Materials Science and Engineering, University of Michigan, 2300 Hayward Street, Ann Arbor, MI 48109-2136, USA

Received 8 November 2001; accepted 11 December 2001

A model automotive-exhaust catalyst, Pd on Zr-rich ceria–zirconia, was characterized by X-ray diffraction, optical and electron microscopies, and micro-Raman spectroscopy following high-temperature aging. A broad bimodal distribution of Pd, introduced amongst the 10-μm spherical particles of support material during catalyst preparation, was found to persist upon aging, and strained PdO was detected predominantly in those particles containing the higher concentration of Pd. The strain, approximately −1% by volume, was determined from the shift of the strong PdO Raman line at 650 cm^{-1} and the Grüneisen parameter, which was measured in a separate experiment in a diamond-anvil cell. The origin of the compressive stress that gives rise to this strain is believed to be the same as in the previously known phenomenon of Pd–metal encapsulation, but the Pd particles involved here are apparently not highly constrained within the sintered ceria–zirconia matrix prior to their oxidation.

KEY WORDS: aging; automotive-exhaust catalyst; ceria–zirconia; encapsulation; Grüneisen parameter; Pd; PdO; strain; Raman spectroscopy; SEM; TEM; XRD.

1. Introduction

Continuous improvement in thermal stability of automotive exhaust catalysts is required in order to steadily achieve ever-lower emission levels that can be maintained throughout the life of the vehicle. It is becoming increasingly important, therefore, to better understand the stages of deactivation, including the detailed mechanisms involved in thermal aging processes. Towards this end, the present study was undertaken to characterize more thoroughly a recently observed catalyst deactivation phenomenon, the deep encapsulation of precious metal by ceria–zirconia support material during high-temperature accelerated aging [1–3]. Under such conditions, as both metal and support sinter, a fraction of the metal particles that form becomes trapped within the ceramic matrix. According to direct observations made by transmission electron microscopy (TEM), these particles are fully constrained, totally inaccessible to gas-phase species, and thus unable to participate in catalytic reactions. In the case of Pd catalysts, the encapsulated metal particles are so tightly held that they exhibit a compressive strain, detectable by X-ray diffraction. Although this final state of the metal particles may be defined, the precise sequence of events preceding it has not yet been determined. In this work, however, a new observation, strained PdO, has been made that suggests the metal particles initially become loosely trapped within the ceria–zirconia before it finally collapses around them to create a fully dense composite. Consequently, before this stage is reached, even more Pd may be lost to catalysis than previously thought.

2. Experimental details

The model catalyst is one of the series studied previously in connection with thermal stability of oxygen storage capacity (OSC) [4]. Briefly, the catalyst was made by impregnation of a commercial-grade ceria–zirconia powder with an aqueous solution of Pd nitrate to incipient wetness, followed by drying at 55 °C for 12 h and calcination at 600 °C for an additional 12 h in a standard muffle furnace. The catalyst was then aged under a laboratory redox cycle designed to simulate air–fuel variations of automotive exhaust. Aging temperature and time were 1050 °C and 12 h, respectively. Specific surface areas were determined by the BET method with a Micromeritics Gemini 2360 surface area analyzer, and powder X-ray diffraction (XRD) data were obtained with a Scintag X1 diffractometer using Cu K_α radiation. The nominal composition, surface areas, crystallographic phases present, cell parameters, and %Pd encapsulated, all previously reported [4], are listed in table 1.

In the present study, the aged catalyst was further characterized by XRD, transmission electron microscopy (TEM), scanning electron microscopy (SEM), optical microscopy, and Raman spectroscopy. The electron microscopy was performed with a JEOL 2010F TEM and a Philips XL30FEG SEM, both of which have field-emission electron sources and X-ray energy dispersive spectroscopy (EDS) capabilities. The Raman spectroscopy was performed with a dual wavelength

* To whom correspondence should be addressed.

1011-372X/02/0400-0099/0

Table 1
Properties of the model Pd/ceria–zirconia catalyst, Pd/ZC2 [4]

Nominal ceria–zirconia composition	20.1 wt% CeO_2 79.9 wt% ZrO_2
Pd loading (wt%)	2
Specific surface areas (m^2/g)	80—fresh 2—aged
Phase [a] (cell parameters (nm)) [b]	t/c, m—fresh t (0.512, 0.522)—aged
%Pd encapsulated	~20—aged

[a] m, monoclinic (ZrO_2); t, tetragonal; c, cubic.
[b] (a, c) of double tetragonal cell.

(UV and visible) Renishaw 1000 microscope system using mainly the 488-nm line from an Ar-ion laser. Spectra were calibrated with the 546.1-nm Hg emission line. Ancillary Raman spectroscopy measurements were also made on PdO crystals, prepared earlier [5], at high pressure using a P-series diamond-anvil cell made by High Pressure Diamond Optics, Inc. For higher resolution, these data were taken using another Renishaw 1000 microscope equipped with a HeNe laser (633-nm excitation line). Ruby crystals for calibrating the pressure were loaded in the cell along with the PdO crystals and a 4:1 methanol:ethanol hydrostatic pressure medium.

3. Results

As reported previously [4], the ceria–zirconia support material is initially a mixture of two crystalline phases, monoclinc and tetragonal. Upon aging, the monoclinic phase disappears, as shown in figure 1, suggesting that

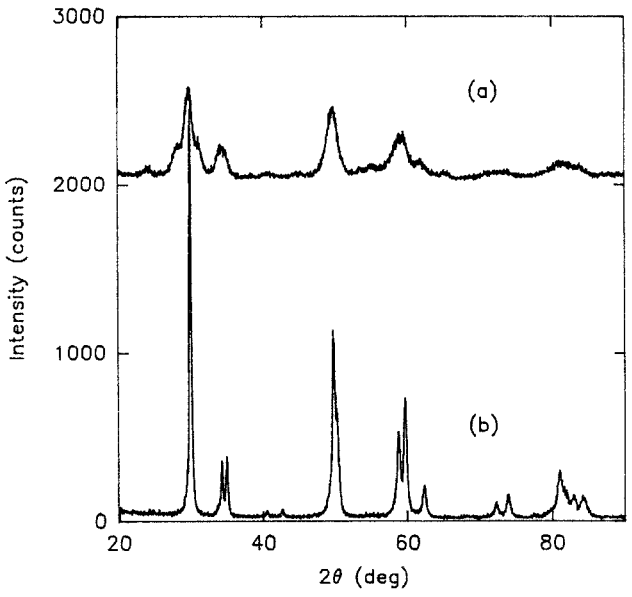

Figure 1. XRD patterns of fresh (a) and aged (b) Pd/ZC2. The peaks in (a) not found in (b) arise from a monoclinic phase.

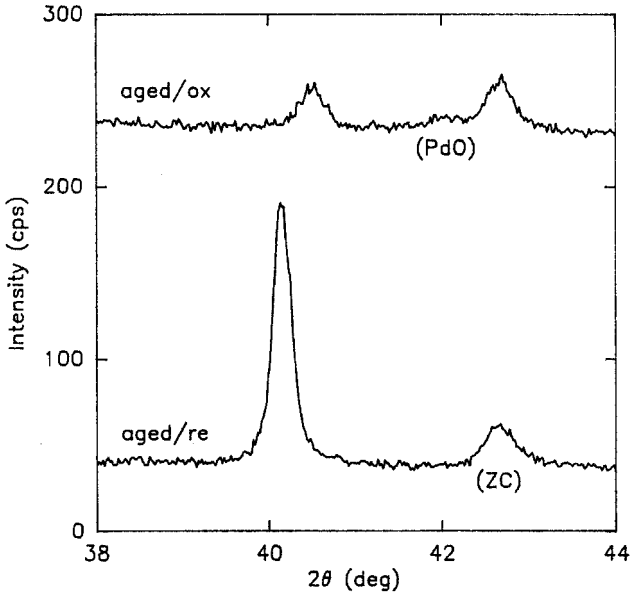

Figure 2. XRD patterns of aged Pd/ZC2 showing structure due to diffraction from encapsulated Pd particles (at 40.6°), PdO, undifferentiated (total) Pd (at 40.1°), and ceria–zirconia (ZC). The labels, aged/ox and aged/re, refer to aged catalysts that were subsequently heated in air at 700 °C for 2 h or in 0.5% H_2 at 500 °C for 0.5 h, respectively. The position of the Pd(111) peak in the upper pattern, arising from the encapsulated Pd particles, corresponds to a compressive strain of approximately 3% by volume.

the catalyst may have become homogeneous. A more accurate determination of the fraction of Pd encapsulated, made by comparing the Pd(111) XRD peak intensities from aged samples that were subsequently oxidized (in order to convert any unencapsulated Pd to PdO) or reduced (in order to remove stress from the encapsulated Pd and convert all PdO to Pd), confirmed the value of 20%, as shown in figure 2. The position of the Pd(111) peak in the upper pattern, approximately 40.6° (2θ), corresponds to a compressive strain of approximately 3% by volume.

An obvious inhomogeneity does exist in the Pd distribution, however, first noticed by optical microscopy in the course of preparing cross-sectional specimens for TEM. As shown in figure 3(a), the aged catalyst powder, following oxidation (performed by heating at 700 °C in air for 2 h), consists of spheres, ranging in diameter from roughly 5 to 20 μm, that vary in color between light and dark gray. When potted in glue and polished, the different colors on the surfaces of individual spheres were found to extend throughout their interiors, as shown in the color image of figure 3(b). The color distribution was distinctly bimodal, *i.e.*, most spheres could be classified as either "light" or "dark". Since the darkness of a catalyst is typically associated with the presence of small metallic particles formed by sintering upon aging, it was initially thought that the difference in color might reflect a difference in the extent of Pd–metal encapsulation. In fact, EDS analysis of several

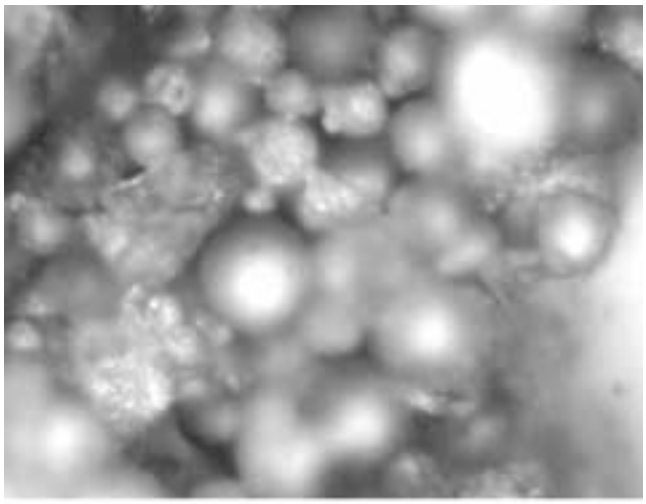

(a)

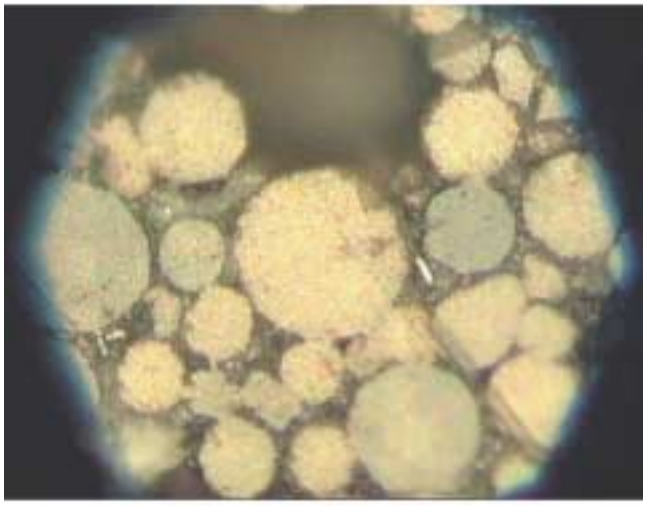

(b)

Figure 3. Optical micrographs of aged Pd/ZC2 in free aggregate form (a) and after potting and polishing (b).

spheres using the SEM (with a beam voltage of 20 kV) revealed an apparent difference in total Pd concentration, as shown in table 2. The cerium and zirconium contents, however, are substantially the same from sphere to sphere. (Note that the ceria–zirconia compositions in tables 1 and 2 do not agree. The error is probably in the SEM-EDS results since they have not been corrected for self-absorption.)

TEM observations were made without reference to the color of the material. Although 20% of the Pd is encapsulated, according to XRD, it was difficult to locate such Pd particles. Occasionally, several would be found together. Some examples are shown in figure 4. The appearance of these Pd particles (size, shape, and disposition in the matrix) resembles that of those observed previously in a Ce-rich catalyst [2].

Table 2
Composition of some representative light and dark spheres obtained by SEM-EDS

Color	Composition (wt%)			
	Zr	Ce	O	Pd
light1	62.3	20.1	16.2	1.4
light2	62.8	20.5	15.7	1.0
light3	62.1	20.9	15.0	2.0
light4	62.0	20.6	15.8	1.6
light5	62.4	20.6	15.5	1.5
light6	62.4	20.4	15.6	1.6
light7	62.2	20.8	15.9	1.1
light8	61.9	19.4	17.1	1.6
light (average)				1.5 ± 0.3
dark1	61.8	19.2	15.8	3.2
dark2	63.0	20.3	15.0	1.7
dark3	61.1	19.1	17.1	2.7
dark4	63.0	21.1	13.4	2.5
dark5	62.2	19.7	14.9	3.2
dark6	62.6	19.9	15.8	1.7
dark7	59.9	20.1	17.6	2.4
dark8	63.0	20.3	14.9	1.8
dark (average)				2.4 ± 0.6

Other possible reasons for the color differences shown in figure 3(b) include differences in the phase composition of the ceria–zirconia matrix or, more likely, the degree of oxidation of the Pd. Raman microscopy is an ideal technique to look for such differences, since it is sensitive to subtle changes in phase and has sufficient spatial resolution (~1 mm) to probe individual spheres without interference from neighboring ones.

Raman spectra of solid solutions of the form $Ce_{1-x}Zr_xO_2$ are very sensitive to the value of x. For $x = 0$ the material has the cubic fluorite structure with a single Raman line at 465 cm^{-1} [6]. For $x \approx 0.85$, which is the approximate value for the matrix in these studies, the structure becomes tetragonal with six lines or a mixture of tetragonal and monoclinic, depending on the processing [7,8]. For $x = 1$, the structure is monoclinic with an even larger number of lines [9]. Palladium oxide (PdO) also has an easily recognized Raman signature, which is a strong B_{1g} mode at 650 cm^{-1}. For detecting trace amounts of PdO, excitation near 2.41 eV is preferred, since PdO shows a resonance enhanced Raman signal peaking at this energy [5]. We use 488 nm excitation (2.54 eV), which is sufficiently close to the resonance condition to still give a strong enhancement.

Figure 5 shows reference spectra for aged ZC2 matrix (without Pd) and a small PdO crystal, along with typical spectra from light and dark spheres. Aside from a difference in overall intensity, again reflecting the difference in color and penetration of the laser, the Raman peaks from the ceria–zirconia matrix in both the light and dark spheres (figures 5(a) and (b)) are identical to those in the reference material shown in figure 5(c). The peaks

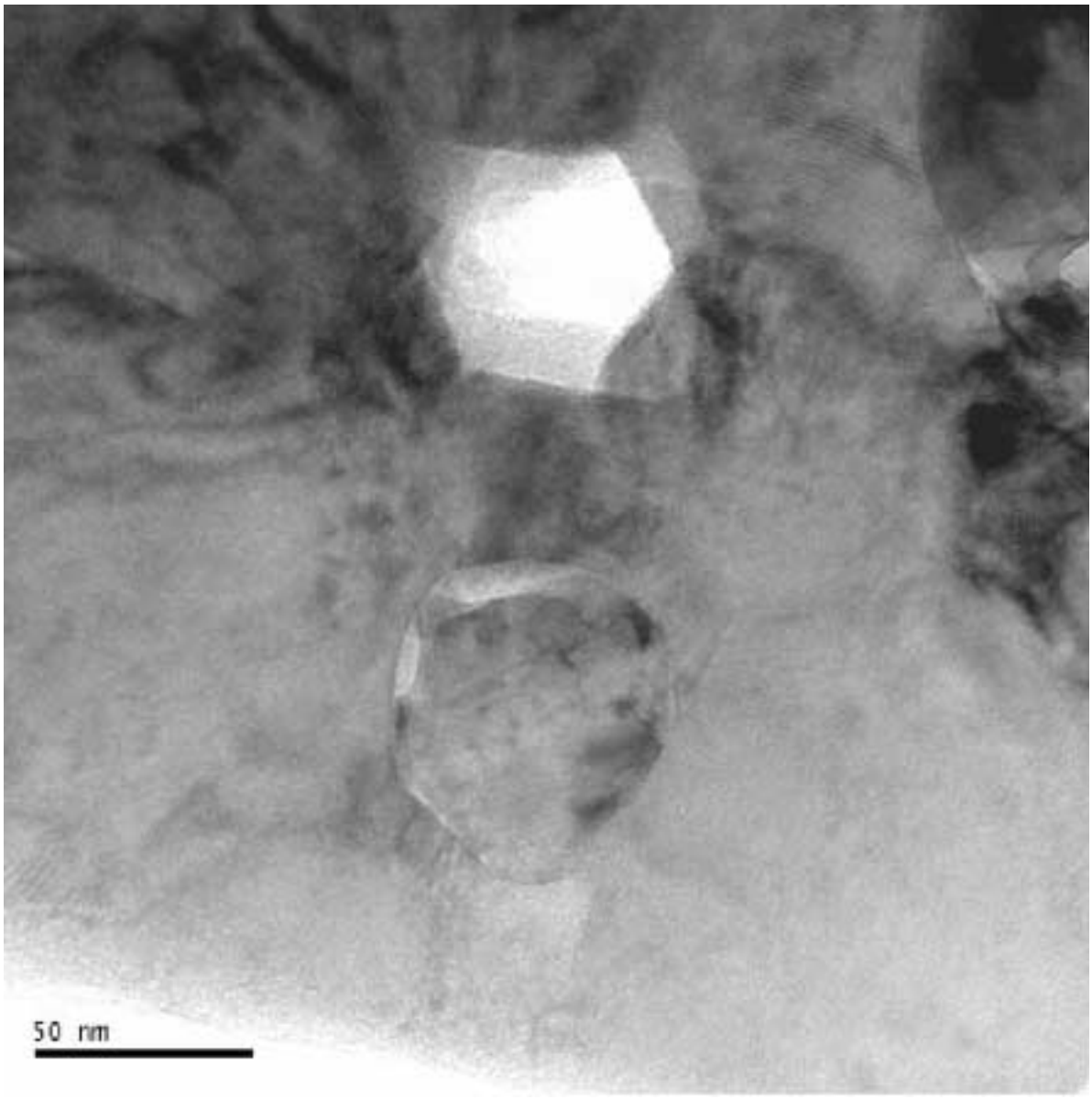

Figure 4. TEM of Pd/ZC2 showing encapsulated Pd particles (upper right corner and bottom center) and a void (top center) within the ceria–zirconia matrix.

at 143, 259, and 313 cm^{-1} identify the matrix as having the tetragonal structure [7]. Thus, there is no difference in this aspect of the catalyst between light and dark spheres. The PdO line, however, is significantly different in the two samples. Figure 6 shows an expanded plot of the 650 cm^{-1} region for a number of light and dark spheres. In the light spheres, this line is stronger and peaks at a lower frequency than it does in the dark spheres. Its asymmetric shape suggests that another peak at a higher frequency may be obscured. The dark spheres clearly show two peaks for this mode, with the stronger peak extending as much as 15 cm^{-1} above the frequency for the reference PdO material, which is indicated by the dashed vertical line. Note that the PdO line in both dark and light spheres is much broader than the same line in the PdO crystal (figure 5).

We attribute the positive frequency shift to compressive strain (as discussed below). The increased width is likely due to inhomogeneous broadening. The sampling volume of the laser contains $\sim 10^2$ Pd particles of the size shown in figure 4, and we would expect some inhomogeneity with such a large number. As a simple way to characterize the strain distribution in the samples, we fit each spectrum in figure 6 with a pair of lines, whose positions, widths, and intensities were optimized by a least-squares method. These results are summarized in figure 7, in which the integrated relative intensity of each line, normalized to unity for each pair of lines, is plotted as a function of its frequency. The filled (open) symbols are for the dark (light) spheres. This plot shows that in the dark spheres most of the PdO is under the maximum strain, with an average frequency

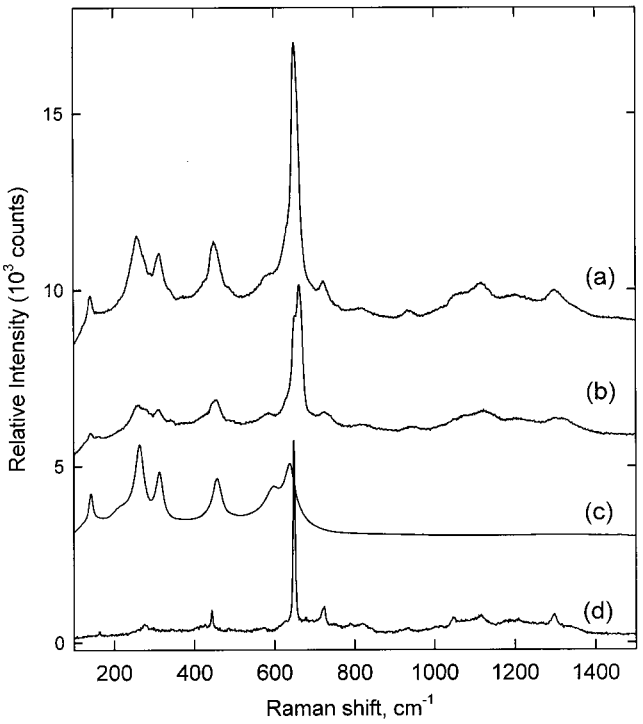

Figure 5. Raman spectra of a light Pd/ZC2 sphere (a), a dark Pd/ZC2 sphere (b), aged ZC2 matrix without Pd (c), and a small PdO crystal (d).

shift of 13.4 cm^{-1}, which is much higher than that in the light spheres. In contrast, most of the PdO in the light spheres is unstrained, and the average maximum shift, 8.6 cm^{-1}, is less than it is in the dark spheres.

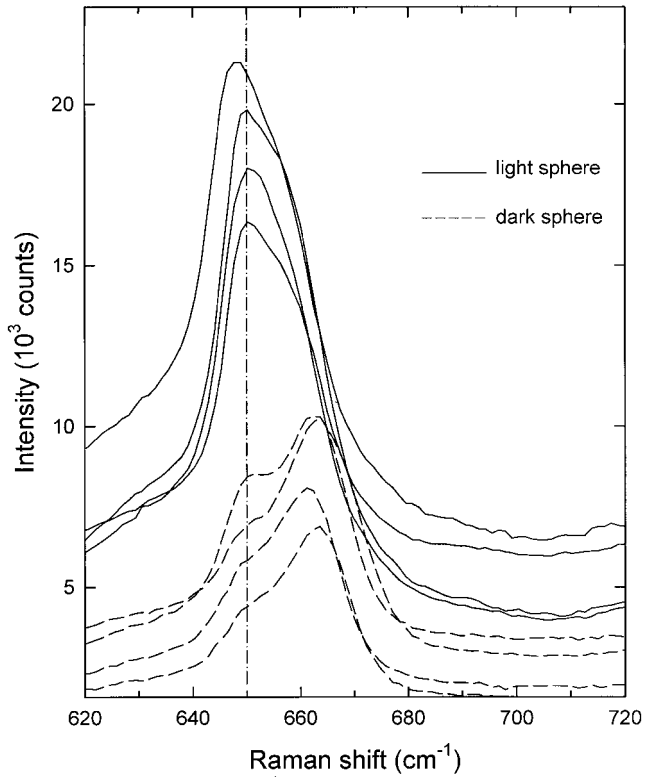

Figure 6. Expanded Raman spectra highlighting the variation of the 650 cm^{-1} PdO line in several light and dark spheres.

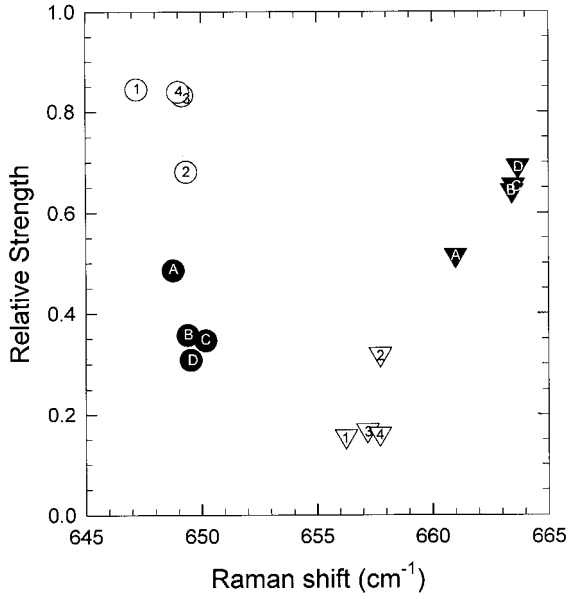

Figure 7. Results of fitting spectra in figure 6 to two Lorentzian lines as explained in the text. Open (filled) symbols represent the light (dark) spheres.

In order to quantify the strain in terms of the Raman frequency, we measured the Raman shift as a function of pressure using a diamond-anvil cell (DAC). The pressures were calculated from the known pressure shift of the R_1 ruby fluorescence line [10]. Figure 8 shows the results from several runs with the DAC. The straight line is a linear least-squares fit. From the slope, we determine the Grüneisen parameter [11], which measures the relative change of the mode frequency with the strain.

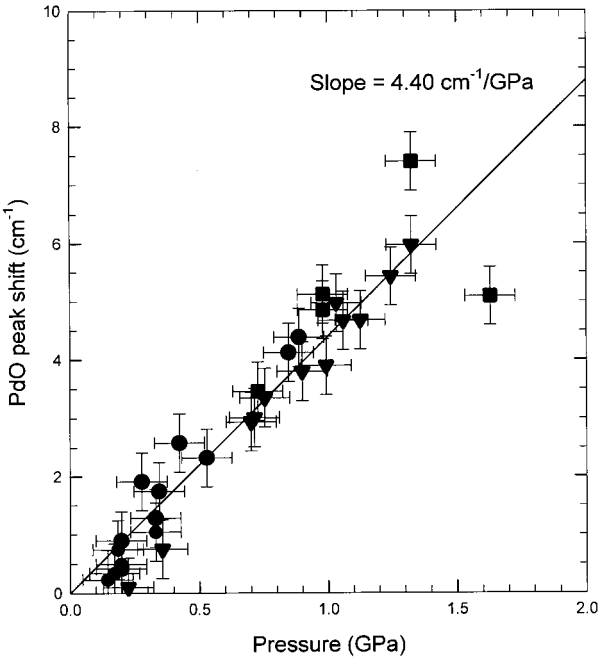

Figure 8. Observed shifts of the 650 cm^{-1} PdO Raman line with pressure measured in a diamond-anvil cell. The straight line is a least-squares fit.

This parameter is defined as

$$\gamma = -\frac{V}{\omega}\frac{\Delta\omega}{\Delta V} = \frac{B_0}{\omega}\frac{\Delta\omega}{\Delta P}, \quad (1)$$

where B_0 is the isothermal bulk modulus, ω is the PdO peak frequency under ambient conditions, and $\Delta\omega$ is the frequency shift. Using $B_0 = 280\,\text{GPa}$ as measured by Christy and Clark [12], our data give $\gamma = 1.9 \pm 0.1$. We then use the above equation to get values for the strain as $\Delta V/V = -0.01$ for the dark spheres ($\Delta\omega = 13.4\,\text{cm}^{-1}$) and -0.007 for the light spheres ($\Delta\omega = 8.6\,\text{cm}^{-1}$). The negative sign indicates compressive strain on the PdO. Note that the magnitude of the strain is too small to be readily observed by XRD, especially in view of the interference between the strongest PdO peaks and those of ceria–zirconia.

4. Discussion

According to the original interpretation of the encapsulation phenomenon, the strain observed in Pd–metal particles is the result of a stress, applied by the encapsulating ceria–zirconia matrix, due primarily to a dimensional change associated with its variable oxygen content [3]. A number of observations have been made subsequently that are not readily explained by this simple description, and one of these, strained PdO, has stimulated another interpretation [13], which is summarized as follows.

Consider an unstrained Pd–metal particle that completely fills a cavity of volume V within a matrix of fully oxidized ceria–zirconia. For simplicity, assume that the bulk modulus of Pd, B, is much smaller than that of ceria–zirconia. If this system is placed in an oxygen-containing atmosphere, its energy can be lowered through oxidation of Pd, since oxygen can readily be transported through the ceria–zirconia in order to react with the metal [14]. As a result, the particle should become larger, because PdO has a lower density than Pd. This growth in particle size, however, is inhibited by the ceria–zirconia matrix. The change in volume due to oxidation, ΔV, would be imposed on the particle, creating a strain that raises the energy of the system by approximately $(B/2)\Delta V^2/V$. The total change in energy is thus given by

$$\Delta E = \Delta G \rho_m k \Delta V + (B/2)\Delta V^2/V, \quad (2)$$

where ΔG is the change in free energy per mole of Pd for the reaction $2\text{Pd} + \text{O}_2 \rightarrow 2\text{PdO}$, ρ_m is the molar density of Pd, and k is a constant that relates the molar volume of Pd to the difference in molar volumes between PdO and Pd. Minimizing this change in energy with respect to ΔV yields the equilibrium value

$$\Delta V/V = \Delta G \rho_m k/B. \quad (3)$$

Although this estimate of $\Delta V/V$ is very crude (*e.g.*, the choice of a single ΔG ignores pressure and temperature variations), it provides good agreement with observations, accounting for the 3% compressive strain shown in figure 2, for example, with $\Delta G = -9\,\text{kcal/mol-Pd}$, $\rho_m = 1.13 \times 10^5\,\text{mol-Pd/m}^3$, $k = 1.46$, and $B = 183\,\text{GPa}$ [13]. Accordingly, if the original Pd particle were spherical, the strained particle would consist of a spherical Pd core surrounded by a PdO shell having a thickness equal to about 2.5% of the particle radius, or about 0.6 nm in the case of a 50-nm Pd particle. This thickness is comparable with the unit cell dimensions of PdO, and the actual presence of such a PdO shell would be difficult to detect, even with TEM [2].

Suppose, however, that the initially unstrained Pd particle does *not* entirely fill the cavity of volume V within the matrix of fully oxidized ceria–zirconia. Specifically, if its volume is only somewhat greater than 60% of V, it can undergo almost complete conversion to PdO before it, too, becomes constrained by the ceria–zirconia. Since the bulk modulus of PdO is larger than that of Pd (by about 50%), the strain that develops should be less than in Pd metal. Using equation (3), but inserting the numerical value of the bulk modulus of PdO rather than Pd, the equilibrium value of $\Delta V/V$ is found to be -0.02, still somewhat larger in magnitude than the observed value of -0.01.

The picture that emerges from this revised model of encapsulation is that the strained Pd–metal particles that are fully constrained by the ceria–zirconia matrix typify just the final stage of a process that involves much more loosely constrained Pd particles that may undergo oxidation (and then reduction) without having direct access to gas-phase oxygen. For a certain range of volume filling factors (from ~60% to somewhat under 100%), strained PdO can also develop due to encapsulation. The fraction of metal that resists oxidation (or develops strain) provides only a lower bound to the total amount that is lost for catalysis. In the case of the dark spheres, for example, ~60% of the Pd *not* contributing to the strained-metal fraction is also encapsulated, but as PdO. If only a small fraction of the Pd particles, on the other hand, are barely constrained as PdO, possibly as in the case of the light spheres, the average strain may not reach the maximum (equilibrium) value, as in figure 7.

A schematic illustration of the various stages of encapsulation is shown in figure 9. The left side of the figure shows catalysts that have been reduced, and the right side shows the effect of oxidation. At a sufficiently early stage of aging, shown at the top of figure 9, where there has not yet been any encapsulation, all of the Pd particles can be transformed into PdO through reaction with gas-phase O_2. Upon further aging, characterized by increased sintering of both Pd and ceria–zirconia, some of the Pd particles have become loosely constrained within pores in the ceria–zirconia, as shown in the

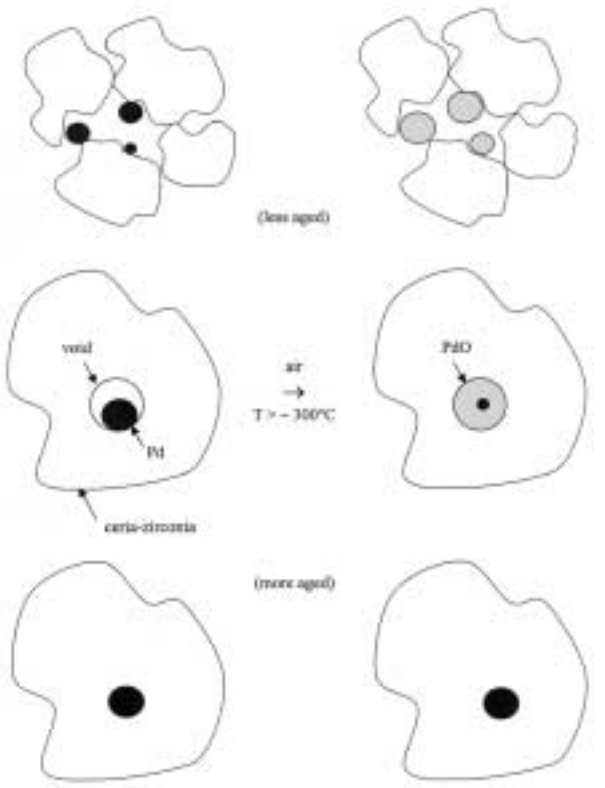

Figure 9. Schematic representation of the early (top), intermediate (middle), and late (bottom) stages of aging in which Pd particles are encapsulated. Reduced samples are on the left, oxidized samples on the right.

middle part of figure 9. These particles can only be oxidized by the oxygen that diffuses through the ceria–zirconia lattice, and if the reaction is limited by the development of strain, some of the Pd is left unoxidized. Such particles would contribute to both the strained-Pd fraction, as seen by XRD, and the strained-PdO fraction, as seen by Raman spectroscopy. Finally, after even more aging, where the surface area of the catalyst has fallen about as far as possible, most of the Pd particles have become fully constrained within the ceria–zirconia matrix, and only a very thin shell of PdO can form around them upon oxidation, as shown at the bottom of figure 9. At this stage, most of the Pd would appear as strained metal.

As discussed before [3], the tendency toward encapsulation is a function of many variables, including aging temperature, metal loading, and ceria–zirconia surface area. In this particular catalyst, it is likely that the support particles that eventually became dark took up more of the Pd precursor during preparation, resulting in higher Pd loading and thus greater tendency toward encapsulation. The origin of this difference in the support material is not known, but it may well be related to the initial phase inhomogeneity of the support. Attempts to observe variation in phase content and possibly correlate this with the differences in color of individual spheres found in the fresh catalyst were not successful, however.

5. Conclusions

The observation of strained PdO together with the realization of its connection to catalyst deactivation by precious-metal encapsulation has two important implications: (1) the loss of Pd through encapsulation is greater than previously realized, and (2) encapsulation may, in general, proceed through a process of shrinking voids in ceria–zirconia support material. Additionally, the ability of Raman microscopy to detect this phenomenon makes it a viable diagnostic tool for the further study of this potentially serious thermal deactivation mode.

Acknowledgments

The work at the University of Michigan was supported by National Science Foundation Grant DMR-9871177 (for the JEOL 2010F TEM, located in the Electron Microbeam Analysis Laboratory) and Ford Motor Company, through a University Research Program grant. Aging treatments were performed by H.-W. Jen.

References

[1] G.W. Graham, H.-W. Jen, W. Chun and R.W. McCabe, Catal. Lett. 44 (1997) 185.
[2] J.C. Jiang, X.Q. Pan, G.W. Graham, R.W. McCabe and J. Schwank, Catal. Lett. 53 (1998) 37.
[3] G.W. Graham, H.-W. Jen, W. Chun and R.W. McCabe, J. Catal. 182 (1999) 228.
[4] G.W. Graham, H.-W. Jen, R.W. McCabe, A.M. Straccia and L.P. Haack, Catal. Lett. 67 (2000) 99.
[5] J.R. McBride, K.C. Hass and W.H. Weber, Phys. Rev. B 44 (1991) 5016.
[6] W.H. Weber, K.C. Hass and J.R. McBride, Phys. Rev. B 48 (1993) 178.
[7] G. Colón, M. Pijolat, F. Valdivieso, H. Vidal, J. Kašpar, E. Finocchio, M. Daturi, C. Binet, J.C. Lavalley, R.T. Baker and S. Bernal, J. Chem. Soc. Faraday Trans. 94 (1998) 3717.
[8] M. Yashima, H. Arashi, M. Kakihana and M. Yoshimura, J. Am. Ceram. Soc. 77 (1994) 1067.
[9] D.R. Clarke and F. Adar, J. Am. Ceram. Soc. 65 (1982) 284.
[10] B.A. Weinstein and R. Zallen, in: *Light Scattering in Solids*, eds. M. Cardona and G. Güntherodt (Springer, Berlin, 1984), Chap. 8.
[11] N.W. Ashcroft and N.D. Mermin, *Solid State Physics* (Holt, Rinehart and Winston, Philadelphia 1976) p. 493.
[12] A.G. Christy and S.M. Clark, Phys. Rev. B 52 (1995) 9259.
[13] G.W. Graham and A.N. Shigapov (submitted for publication).
[14] M.Yu. Smirnov and G.W. Graham, Catal. Lett. 72 (2001) 39.